ChemComm

COMMUNICATION

View Article Online
View Journal | View Issue

Cite this: *Chem. Commun.*, 2020, **56**, 289

Received 20th September 2019,
Accepted 25th November 2019

DOI: 10.1039/c9cc07407d

rsc.li/chemcomm

Optical pico-biosensing of lead using plasmonic gold nanoparticles and a cationic peptide-based aptasensor†‡

Manju Solra,§[a] Rajni Bala,§[a] Nishima Wangoo,*[b] Gurpreet K. Soni,[a] Munish Kumar[a] and Rohit K. Sharma*[a]

A novel biosensor for the rapid detection of lead ions employing the optical properties of AuNPs, a lead-specific aptamer and a cationic peptide has been demonstrated. The limit of detection of the biosensor was 98.7 pM, the lowest so far obtained using colorimetry.

The use of certain heavy metals such as iron, cobalt, cadmium, copper, nickel, zinc, *etc.* is important for biological and environmental applications.[1] But they are generally not tolerated well at high concentrations, and some of the them, such as lead, mercury, and cadmium, are toxic even at relatively low concentrations.[2] Moreover, Pb^{2+} ions are present in substantial amounts in the environment, largely due to the result of human activities such as smelting, mining, internal and topical medicinal preparations, and cosmetic and paint preparations.[3] The World Health Organization (WHO) has set the maximum permissible limit (MPL) of Pb^{2+} ions in drinking water to be 72 nM.[4] Traces of Pb^{2+} ions, *i.e.*, when even just a bit above the permissible limit, have been reported to result in fatal diseases such as cancer, cardiovascular disorders, brain disease, and failures of the kidneys and nervous system.[5,6] Thus, considering the serious complications arising due to the presence of Pb^{2+} ions, it is essential to develop a simple and rapid method for detecting them with high specificity and sensitivity.

Several analytical methods based on atomic absorption spectrometry (AAS),[7] mass spectrometry (MS),[8] atomic emission spectrometry (AES),[9] electrochemistry,[10] and stripping voltammetry[11] have been reported to be employed for detecting Pb^{2+} ions. Though these techniques are fairly sensitive and precise, they suffer from certain limitations such as requiring a trained staff, high-end instrumentation, sophisticated handling, relatively high cost, and a time-consuming procedure limiting their use for rapid and on-site monitoring of Pb^{2+} ions.

These issues can be effectively countered by using the simple yet sensitive colorimetric method, which allows for a direct determination of the target content by observing a change in color with the naked eye.[12] Such colorimetric methods have been employed for detecting toxic gases,[13] pesticides[14–16] and biomolecules.[17] For this purpose, gold nanoparticles (AuNPs) have been extensively used for colorimetric biosensing of various targets since these NPs have large surface areas, extremely good optical properties, and high molar extinction coefficients, and since their surfaces can be modified in a variety of ways.[18–20] Moreover, AuNPs display distinct color changes and SPR peak shifts that depend on their shape, size and aggregation state, features making them relatively reliable sensors.[21] All of these properties make AuNPs a strong contender for ultra-sensitive biosensing.[22,23]

In addition to AuNPs, aptamers have also shown promise in the field of sensing. Aptamers are single-stranded RNA/DNA molecules that bind to specific targets with high specificity and selectivity levels.[24] They have emerged as a promising class of recognition elements as a result of their numerous advantages over other entities.[25] The unique properties of aptamers such as their high thermostability, low immunogenicity, low toxicity, remarkable affinity, and easy synthesis and modification have attracted much attention, making them desirable recognition elements for sensing applications.[26] Electrochemical aptasensors have been reported to be constructed for the detection of Pb^{2+} ions, but their limit of detection (LOD) values were observed to be not very low.[27] Moreover, a rapid and on-site detection of Pb^{2+} ions in real samples is not possible using an electrochemical apparatus.

Due to the above-described complexities involving instrumentation and reagent selection for the detection of small amounts of metal ion, in the current work we set out to develop a simple, cost-effective, rapid, sensitive and label-free colorimetric biosensor of lead ions using a novel strategy employing AuNPs, an aptamer, and a cationic peptide. The developed

[a] *Department of Chemistry and Centre of Advanced Studies in Chemistry, Panjab University, Sector-14, Chandigarh 160014, India. E-mail: rohitksg@pu.ac.in*
[b] *Department of Applied Sciences, University Institute of Engineering and Technology (U.I.E.T.), Panjab University, Sector-25, Chandigarh 160014, India. E-mail: nishima@pu.ac.in*

† This communication is dedicated to Prof. D. V. S. Jain, Professor Emeritus, Department of Chemistry, Panjab University, India who passed away on 7th October 2019.

‡ Electronic supplementary information (ESI) available. See DOI: 10.1039/c9cc07407d

§ Contributed equally.

assay for detecting lead showed an LOD in the picomolar range, better than any LOD so far reported according to a survey of the latest literature.

The principle of the developed sensing system was based on aggregation of AuNPs inducing a change in the color of the tested solution from wine red to blue with a subsequent change in the absorption spectrum.

Furthermore, the designed sensor system was observed to be highly selective when tested in the presence of other metal ions as well as in real samples.

The primary objective of the work was to detect Pb^{2+} ions, owing to their pernicious effects, with a simple, rapid, cost-effective and reliable method. The design of the present sensing assay was based on AuNPs, a Pb^{2+}-specific aptamer, and a cationic hexapeptide. The AuNPs (0.2166×10^{-8} mol L^{-1}), owing to their distinct color responses associated with different aggregation states, were found to serve as excellent optical indicators for signaling the presence or absence of the target analyte (Pb^{2+} ions in the present case). The synthesis of AuNPs was carried out *via* a chemical methodology that employed trisodium citrate as a capping as well as reducing agent. The AuNPs formed were negatively charged and stable as a result of electrostatic repulsions between the citrate ions (capping agent) present on the AuNP surfaces. The sequence of the peptide (KRKRKR-amide) was selected to be sufficiently cationic to induce the aggregation of AuNPs through electrostatic interactions (Fig. S4, ESI‡), and to facilitate its electrostatic binding with a negatively charged aptamer.

The mechanistic principle of the colorimetric aptasensor for Pb^{2+} ions is illustrated in Fig. 1. The specific binding of the aptamer with Pb^{2+} ions was exploited in order to develop a highly sensitive colorimetric biosensor. The aptamer was found to specifically bind with any present Pb^{2+} ions (Fig. S5, ESI‡), leaving the cationic peptide free in the solution (Fig. 1A). Consequently, the availability of sufficient peptide in the solution resulted in the aggregation of the AuNPs, and a distinct color change from wine red to blue was observed. The electrostatic interaction between the negatively charged AuNPs and cationic peptide was responsible for inducing color changes in the gold colloids from red to blue, and these changes were clearly visible with the naked eye. However, in the absence of Pb^{2+} ions, the aptamer bound to the peptide *via* electrostatic interactions (Fig. S6, ESI‡) and rendered the AuNPs well dispersed due to the lack of peptide molecules in the solution; thereby the color of the colloid remained unchanged (red) (Fig. 1B). The extent of aggregation depended on the number of free peptide molecules in the solution: the higher the concentration of Pb^{2+} ions, the greater the number of free peptide molecules and the greater the aggregation. This aggregation through its effect on the color of the solution was easily visualized by the naked eye.

The sensitivity of the developed sensing assay was found to depend on various reaction parameters such as concentration of peptide, concentration of aptamer, incubation time, *etc.* The effect of these parameters was optimized thoroughly. Due to the critical dependence of the aggregation of AuNPs on the concentration of cationic peptide, the minimum concentration of peptide sufficient to aggregate the AuNPs was determined. For this purpose, AuNPs were exposed to various concentrations of peptide (ranging from 1 μM to 50 μM) in the presence of phosphate buffer (pH = 7.4), and the absorption spectra of the AuNPs were recorded. For peptide concentrations between 1 μM to 10 μM, the color of the AuNPs remained red with an absorption peak at a wavelength of 520 nm (Fig. 2a), which is the characteristic peak of AuNPs. As the concentration of the peptide was increased to 50 μM, the color of the AuNPs turned blue and a new absorption peak emerged at 650 nm (Fig. 2a), representing the peak of aggregated AuNPs. Therefore, 50 μM was chosen as the peptide concentration for further detection experiments.

After successfully optimizing the concentration of peptide, we set out to determine the minimum concentration of aptamer

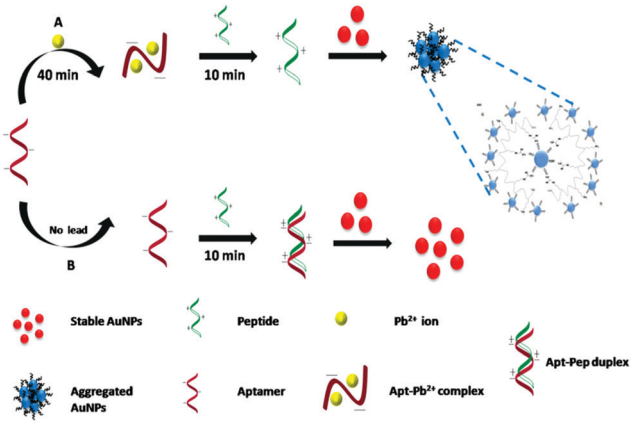

Fig. 1 Detailed schematic illustration of the principle of the detection of lead ions using the developed aptasensor. All depicted reactions were performed at ambient temperature in the presence of phosphate buffer at pH 7.4. The presence of lead ions changed the colour of the solution from red to blue due to the presence of free peptide whereas in the absence of lead ions, the colour of solution remained red.

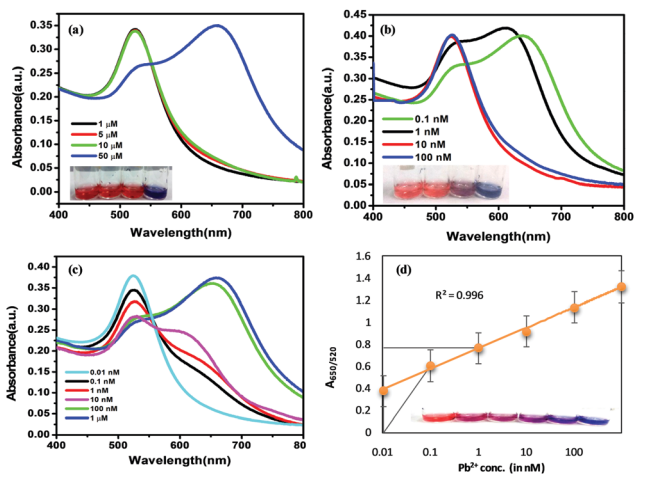

Fig. 2 (a and b) Absorbance spectra of AuNPs in the presence of various concentrations of (a) peptide and (b) aptamer. (c) Absorbance spectra of AuNPs in the presence of lead ion concentrations between 0.01 nM and 1 mM. (d) The intensity ratio $A_{650/520}$ as a function of Pb^{2+} concentration.

needed for binding the peptide to a sufficient extent to keep the AuNPs well dispersed and red in color. Various aptamer samples, each at a different concentration between 0.1 nM to 100 nM, were incubated with 50 μM of cationic peptide and buffer (pH = 7.4) followed by the addition of AuNPs. The absorption spectra of the nanoparticles revealed that, at the lower concentrations of aptamer (0.01 nM and 1 nM), the plasmonic band at 650 nm corresponding to the aggregation of the nanoparticles was relatively prominent (Fig. 2b). This result may be attributed to the amount of aptamer not being enough for binding the peptide, and as a result, the color of the AuNPs turned blue. However, as the concentration of aptamer was increased to 10 nM and above, it completely bound the peptide and hence prevented the aggregation of nanoparticles, as confirmed by the characteristic plasmon band of AuNPs observed at 520 nm (Fig. 2b). Hence, an aptamer concentration of 10 nM was chosen for further analysis.

Following the successful optimizations of the above-mentioned reaction parameters, the analytical performance of the proposed aptasensor was tested carefully. In order to investigate the sensitivity of the colorimetric biosensor, various concentrations of lead nitrate ranging from 0.01 nM to 1 μM were evaluated. It was observed that as the concentration of lead ions was increased, the absorbance of the AuNPs at 520 nm started to decrease while the intensity of the band at 650 nm increased (Fig. 2c). Additionally, the gradual increase in the concentration of lead resulted in a change in the color of the solution from wine red to purple and then to blue. The results of the assay clearly demonstrated the ability to qualitatively detect Pb^{2+} ions easily and rapidly with the naked eye and without the use of sophisticated instrumentation.

Furthermore, a quantitative estimation of Pb^{2+} ion concentration was carried out by producing a calibration curve. This curve was obtained by plotting the ratio of the absorbance peak intensity at 650 nm to that at 520 nm ($A_{650/520}$) as a function of Pb^{2+} concentration, and found to be highly linear (R^2 = 0.9965) between Pb^{2+} concentrations of 0.01 nM to 1 μM (Fig. 2d). The limit of detection of the developed biosensor was obtained by using the formula LOD = 3α/slope[28,29] and was found to be 98.7 pM (calculation S1, ESI‡), markedly lower than that using any other method reported so far for the detection of Pb^{2+} ions (Table 1).

In order to check the specificity of the developed sensing system for Pb^{2+} ions, interference studies for other metal ions were carried out. These studies included controlled reactions in the presence of different metal ions such as copper, calcium, mercury, zinc, nickel, sodium, potassium and cadmium. These metal ions were chosen because of their presence with Pb^{2+} in the environment and the possibility of their interfering with the detection of Pb^{2+} ions. The results clearly showed the developed colorimetric sensor to be highly specific and selective for Pb^{2+} ions, (Fig. 3a). The aggregation was observed only in case of Pb^{2+} even when the concentration of interfering ions was 10-fold higher than that of the lead ions (Fig. 3a). Moreover, all of the solutions with interfering ions remained red in color whereas in the case of lead ions, the solution changed from red to blue.

Furthermore, the plasmonic peak was observed at 520 nm for all tested potentially interfering ions whereas lead ions showed the peak at 650 nm (Fig. S7, ESI‡). This result confirmed the high specificity and selectivity of the developed colorimetric aptasensor for lead ions. In order to check the potential application of the proposed biosensor, it was further tested in real samples. Water samples were collected from two different sources, namely mineral water (Fig. 3b and Fig. S9, ESI‡) and tap water (Fig. 3c and d). The collected samples were filtered to remove suspended impurities followed by spiking them with known concentrations of Pb^{2+} ions (0.01 nM to 1 μM). The results showed absence of Pb^{2+} ions up to permissible limits as prescribed by WHO.[4] The samples spiked with known concentrations of Pb^{2+} ions were tested with the proposed colorimetric aptasensor. After applying the AuNPs nanoprobe, a linear calibration curve was plotted and the results obtained were compared with the quantity of lead ions added. The results from the designed probe revealed excellent synchronization with the quantity of Pb^{2+} ions added (Table S1, ESI‡). Furthermore, the selectivity of the lead aptamer for lead ions in the presence of other interfering metal ions, such as Pb^{2+} and Cd^{2+}, Pb^{2+} and Hg^{2+}, Pb^{2+} and Zn^{2+}, Pb^{2+} and Cu^{2+}, Pb^{2+} and Ca^{2+}, and Pb^{2+} and Ni^{2+} was investigated (Fig. S8, ESI‡). The lead aptamer was clearly observed to be specific for lead ions in the presence of the tested interfering ions. These results validated the

Table 1 Comparison of the currently developed aptasensor method with methods reported in the literature for lead detection

Technique	Limit of detection	Ref.
Electrochemical	5 nM	30
Fluorescence	4.6 nM	31
Colorimetric	0.1 nM	32
Ratiometric	1 nM	33
Magneto-elastic biosensor	0. 3 μM	34
Colorimetric	**98.7 pM**	**Present method**

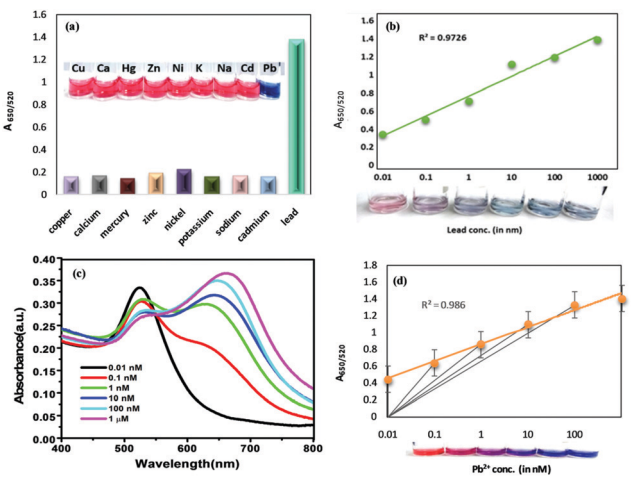

Fig. 3 (a) Histogram of the selectivity of the aptasensor towards lead ions. (b) Calibration curve of the response to various concentrations of lead ions in mineral water. (c) UV-Vis spectra of the aptasensor tested in real samples (tap water). (d) Quantitative analysis showing the effect of the developed biosensor in tap water.

practical application of the proposed biosensor, and showed that it can be further commercially developed for the detection of lead ions.

In summary, in the current work, a novel AuNP-based colorimetric aptasensor was designed and tested, and showed selective, sensitive and reliable detection of Pb^{2+} ions. The LOD of the proposed biosensor was observed to be 98.7 pM for Pb^{2+} ions, the best reported so far using colorimetry. In the absence of Pb^{2+} ions, the cationic peptide interacted electrostatically with the Pb^{2+}-specific aptamer, and as a result, the AuNPs retained their dispersity and red color. Addition of Pb^{2+} ''turned on'' the aptasensor and its color changed from wine red to blue owing to the presence of free peptide, which aggregated the AuNPs. Moreover, the SPR peak showed a red shift from 520 nm to 650 nm, which further confirmed that Pb^{2+} ions were detected. The Pb^{2+} ion concentration was quantitatively determined in the range of 0.01 nM to 1 μM with a high determination coefficient. The method employed the optical properties of AuNPs, cationicity of the hexapeptide, and specificity of the aptamer. The aptamer provided high specificity and selectivity to the assay, with the aptamer changing its conformation upon binding the target. The sensor array was demonstrated to be highly selective for Pb^{2+} ions as compared to other metal ions such as copper, calcium, mercury, zinc, nickel, sodium, potassium and cadmium. Exposure of the aptasensor to spiked tap water produced the desired results. Thus, the developed aptasensor allows the simple, rapid detection of trace amounts of Pb^{2+} ions with high specificity and with the use of inexpensive portable devices. This aptasensor has tremendous potential for applications in actual samples due to its cost-effective nature and rapid colorimetric detection. Such an ultrasensitive optical biosensor can be further used for diverse applications including environmental monitoring, food safety tests, health monitoring and diagnosis.

This work was supported by the Science Engineering and Research Board (SERB), India grant no. EMR/2016/007967 and DST-Purse II grant. RB and GKS thank UGC, India for their respective research fellowships.

Conflicts of interest

There are no conflicts to declare.

Notes and references

1 P. B. Tchounwou, C. G. Yedjou, A. K. Patlolla and D. J. Sutton, *EXS*, 2012, **101**, 133–164.
2 M. A. Hossain, P. Piyatida, J. A. T. Da Silva and M. Fujita, *J. Bot.*, 2012, 1–37.
3 P. A. Meyer and M. J. Brown, *Mutat. Res.*, 2008, **659**, 166–175.
4 US Environmental Protection Agency, EPS, Health effects notebook for hazardous air pollutants-draft, EPA-452 D-95-00, PB95-503579, Office of air quality planning and standards. Research Triangle Park, NC 1994.
5 S. Tong, Y. E. V. Schirnding and T. Prapamonto, *Bulletin of the WHO*, 2000, **9**, 78.
6 A. Gambelunghe, G. Sallsten, Y. Borné, N. Forsgard, B. Hedblad, P. Nilsson, B. Fagerberg, G. Engström and L. Barregard, *Environ. Res.*, 2016, **149**, 157–163.
7 H. Tinas, N. Ozbek and S. Akman, *Spectrochim. Acta, Part B*, 2018, **140**, 73–75.
8 E. Skrzydlewsk, M. Balcerzak and F. Vanhaecke, *Anal. Chim. Acta*, 2003, **479**, 191–202.
9 K. S. Rao, T. Balaji, T. P. Rao, Y. Babu and G. R. K. Naidu, *Spectrochim. Acta, Part B*, 2002, **57**, 1333–1338.
10 M. Dali, K. Zinoubi, A. Chrouda, S. Abderrahmane, S. Cherrad and N. J. Jaffrezic-Renault, *Electroanal. Chem.*, 2018, **813**, 9–19.
11 X. Luo, W. Huang, Q. Shi, W. Xu, Y. Luan, Y. Yang, H. Wang and W. Yang, *RSC Adv.*, 2017, **7**, 16033–16040.
12 H. Zhai, Y. Bai, J. Qin and F. Feng, *Sensors*, 2019, **19**, 674.
13 P. Tang and G. Sun, *Sens. Actuators, B*, 2018, **261**, 178–187.
14 R. Bala, A. Swami, I. Tabujew, K. Peneva, N. Wangoo and R. K. Sharma, *Biosens. Bioelectron.*, 2018, **104**, 45–49.
15 R. Bala, R. K. Sharma and N. Wangoo, *Sens. Actuators, B*, 2015, **210**, 425–430.
16 R. Bala, S. Mittal, R. K. Sharma and N. Wangoo, *Spectrochim. Acta, Part A*, 2018, **196**, 268–273.
17 Q. Nie, Y. Zhang, J. Zhang and M. J. Zhang, *Mater. Chem.*, 2006, **16**, 546–549.
18 K. L. Kelly, E. Coronado, L. L. Zhao and G. C. Schatz, *J. Phys. Chem. B*, 2003, **107**, 668–677.
19 M. Bajaj, S. K. Pandey, N. Wangoo and R. K. Sharma, *ACS Biomater. Sci. Eng.*, 2018, **4**, 739–747.
20 K. Bansal, M. Aqdas, M. Kumar, R. Bala, S. Singh, J. N. Agrewala, O. P. Katare, R. K. Sharma and N. Wangoo, *Bioconjugate Chem.*, 2018, **29**, 1102–1110.
21 M. Kumar, W. Tegge, N. Wangoo, R. Jain and R. K. Sharma, *Biophys. Chem.*, 2018, **237**, 38–46.
22 C. Zhang, C. Kong, Q. Liu and Z. Chen, *Analyst*, 2019, **144**, 1205.
23 J. Piao, Q. Zhao, D. Zhou, W. Peng, W. Gao, M. Chen, G. Shu, X. Gong and J. Chang, *Anal. Chim. Acta.*, 2019, **1052**, 145–152.
24 J. M. Liu and X. P. Yan, *J. Anal. At. Spectrom.*, 2011, **26**, 1191–1197.
25 P. Röthlisberger, C. Gasse and M. Hollenstein, *Int. J. Mol. Sci.*, 2017, **18**, 2430.
26 R. Bala, S. Dhingra, M. Kumar, K. Bansal, S. Mittal, R. K. Sharma and N. Wangoo, *J. Chem. Eng.*, 2017, **311**, 111–116.
27 L. Yu, P. Zhang, H. Dai, L. Chen, H. Ma, M. Lin and D. Shen, *RSC Adv.*, 2017, **7**, 39611–39616.
28 S. H. Baek, S. W. Lee, E. J. Kim, D. H. Shin, S. W. Lee and T. J. Park, *ACS Omega*, 2017, **2**, 988–993.
29 A. Kumar, M. Bhatt, G. Vyas, S. Bhatt and P. Pau, *ACS Appl. Mater. Interfaces*, 2017, **9**, 17359–17368.
30 C. Lei, S. Zhang and S. Zha, *Int. J. Electrochem. Sci.*, 2017, **12**, 4856–4866.
31 Y. Liu, Q. Zhou, Y. Yuan and Y. Wu, *Carbon*, 2017, **115**, 550–560.
32 Y. Xiahou, P. Zhang, J. Wang, L. Huang and H. Xi, *J. Mater. Chem. C*, 2018, **6**, 637–645.
33 S. Kaviya, *J. Lumin.*, 2018, **195**, 209–215.
34 X. Guo, S. Sang, A. Jian, S. Gao, Q. Duan, J. Ji, Q. Zhang and W. Zhang, *Sens. Actuators, B*, 2018, **256**, 318–324.

